An Evolutionarily Conserved Mechanism Delimiting SHR Movement Defines a Single Layer of Endodermis in Plants

Hongchang Cui, *et al.*

Science **316**, 421 (2007);
DOI: 10.1126/science.1139531

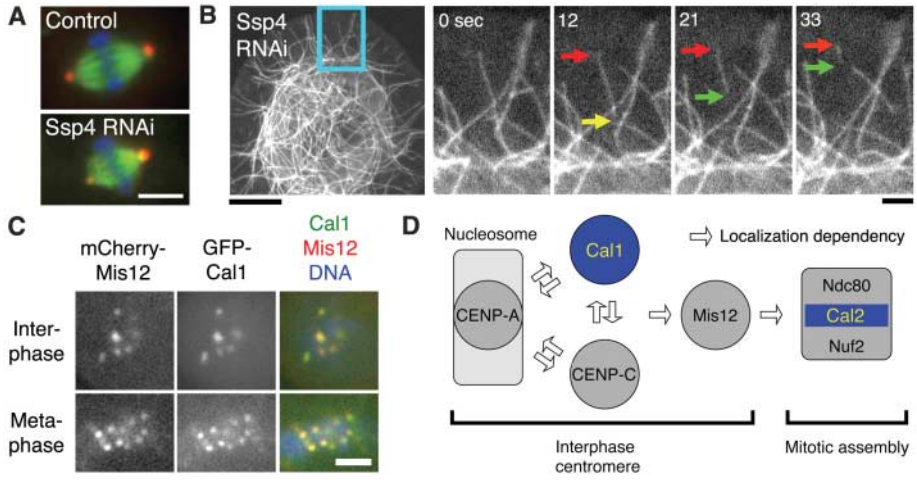

Fig. 4. Regulation of spindle length and chromosome alignment. (**A**) Spindle length was altered after RNAi depletion of the novel protein Ssp4. Scale bar, 5 μm. (**B**) MT severing (yellow arrow) frequently occurred after Ssp4 RNAi. Severed MTs often showed treadmilling behavior (red and green arrows) and then disappeared. Scale bars, 10 μm (left), 2 μm (right). See also movie S4. (**C**) Previously unknown Cal1 protein localizes to the centromere (marked by mCherry-Mis12). (Localization data for other proteins are in fig. S7). Scale bar, 2 μm. (**D**) Model for kinetochore assembly in S2 cells based on protein localization and RNAi. (Data are in fig. S7, D to F).

4. S. Gadde, R. Heald, *Curr. Biol.* **14**, R797 (2004).
5. J. M. Scholey, I. Brust-Mascher, A. Mogilner, *Nature* **422**, 746 (2003).
6. M. Yanagida, *Trends Cell Biol.* **8**, 144 (1998).
7. K. F. Doheny *et al.*, *Cell* **73**, 761 (1993).
8. K. Nasmyth, *Science* **297**, 559 (2002).
9. M. Bettencourt-Dias *et al.*, *Nature* **432**, 980 (2004).
10. B. Sonnichsen *et al.*, *Nature* **434**, 462 (2005).
11. Materials and methods are available as supporting material on *Science* Online.
12. S. L. Rogers, U. Wiedemann, N. Stuurman, R. D. Vale, *J. Cell Biol.* **162**, 1079 (2003).
13. G. Goshima, R. D. Vale, *J. Cell Biol.* **162**, 1003 (2003).
14. Y. Ma, A. Creanga, L. Lum, P. A. Beachy, *Nature* **443**, 359 (2006).
15. M. M. Kulkarni *et al.*, *Nat. Methods* **3**, 833 (2006).
16. N. M. Mahoney, G. Goshima, A. D. Douglass, R. D. Vale, *Curr. Biol.* **16**, 564 (2006).
17. R. Basto *et al.*, *Cell* **125**, 1375 (2006).
18. K. Li, T. C. Kaufman, *Cell* **85**, 585 (1996).
19. J. Luders, U. K. Patel, T. Stearns, *Nat. Cell Biol.* **8**, 137 (2006).
20. H. Muller, M. L. Fogeron, V. Lehmann, H. Lehrach, B. M. Lange, *Science* **314**, 654 (2006).
21. S. Morales-Mulia, J. M. Scholey, *Mol. Biol. Cell* **16**, 3176 (2005).
22. R. D. Saunders, M. C. Avides, T. Howard, C. Gonzalez, D. M. Glover, *J. Cell Biol.* **137**, 881 (1997).
23. S. M. Fung, G. Ramsay, A. L. Katzen, *Development* **129**, 347 (2002).
24. H. Maiato, C. L. Rieder, A. Khodjakov, *J. Cell Biol.* **167**, 831 (2004).
25. G. Goshima, R. Wollman, N. Stuurman, J. M. Scholey, R. D. Vale, *Curr. Biol.* **15**, 1979 (2005).
26. V. I. Rodionov, G. G. Borisy, *Science* **275**, 215 (1997).
27. P. Meraldi, A. D. McAinsh, E. Rheinbay, P. K. Sorger, *Genome Biol.* **7**, R23 (2006).
28. R. Bharadwaj, W. Qi, H. Yu, *J. Biol. Chem.* **279**, 13076 (2004).
29. L. Giot *et al.*, *Science* **302**, 1727 (2003).
30. G. K. Chan, S. T. Liu, T. J. Yen, *Trends Cell Biol.* **15**, 589 (2005).
31. A. Desai *et al.*, *Genes Dev.* **17**, 2421 (2003).
32. K. Takahashi, H. Yamada, M. Yanagida, *Mol. Biol. Cell* **5**, 1145 (1994).
33. M. D. Blower, M. Nachury, R. Heald, K. Weis, *Cell* **121**, 223 (2005).
34. Z. Storchova, D. Pellman, *Nat. Rev. Mol. Cell Biol.* **5**, 45 (2004).
35. E. A. Nigg, *Nat. Rev. Cancer* **2**, 815 (2002).
36. K. W. Yuen, B. Montpetit, P. Hieter, *Curr. Opin. Cell Biol.* **17**, 576 (2005).
37. We thank K. Pollard for valuable suggestions on statistics; Y. Guo, I. Vasenkova, and R. De Breuil for help in dsRNA synthesis at Open Biosystems Inc.; I. Cheeseman for advice on homology searches; A. Straight for sharing data in advance of publication; and S. Henikoff, M. Bettencourt-Dias, D. Glover, T. Kaufman, D. Agard, R. Tsien, and E. Griffis for reagents. G.G. received support from the Human Frontier Science Program and R.W. from a University of California GREAT Training Grant. We thank the Sandler Foundation (UCSF) for support.

Supporting Online Material
www.sciencemag.org/cgi/content/full/1141314/DC1
Materials and Methods
Figs. S1 to S7
Tables S1 and S2
References
Movies S1 to S5
Web site S1

14 February 2007; accepted 23 March 2007
Published online 5 April 2007;
10.1126/science.1141314
Include this information when citing this paper.

An Evolutionarily Conserved Mechanism Delimiting SHR Movement Defines a Single Layer of Endodermis in Plants

Hongchang Cui,[1] Mitchell P. Levesque,[1]*† Teva Vernoux,[1]*‡ Jee W. Jung,[1] Alice J. Paquette,[1] Kimberly L. Gallagher,[1]§ Jean Y. Wang,[1] Ikram Blilou,[2] Ben Scheres,[2] Philip N. Benfey[1]‖

Intercellular protein movement plays a critical role in animal and plant development. SHORTROOT (SHR) is a moving transcription factor essential for endodermis specification in the *Arabidopsis* root. Unlike diffusible animal morphogens, which form a gradient across multiple cell layers, SHR movement is limited to essentially one cell layer. However, the molecular mechanism is unknown. We show that SCARECROW (SCR) blocks SHR movement by sequestering it into the nucleus through protein-protein interaction and a safeguard mechanism that relies on a SHR/SCR-dependent positive feedback loop for *SCR* transcription. Our studies with *SHR* and *SCR* homologs from rice suggest that this mechanism is evolutionarily conserved, providing a plausible explanation why nearly all plants have a single layer of endodermis.

Stem cell renewal and patterned differentiation of their progeny are fundamental processes in the development of multicellular organisms. The root of *Arabidopsis thaliana* is particularly suitable to study these processes, because it has a simple and stereotyped cellular organization (fig. S1) (*1*). SHR and SCR are key regulators of root radial patterning (*2*, *3*) and stem cell maintenance (*4*). In *shr* and *scr* mutants, the cortex/endodermis initial (CEI) cell, which normally gives rise to two files of ground-tissue cells (an inner layer of endodermis and an outer layer of cortex), produces only a single cell layer (fig. S1) (*2*, *3*, *5*). SHR is a transcription factor (*6*) expressed in the stele that moves into the adjacent cell layer where it controls *SCR* transcription and endodermis specification (*6*). By contrast, the SCR protein is absent from the stele, is predominantly expressed in the endodermis, the CEI cell,

[1]Department of Biology and Institute for Genome Sciences and Policy, Duke University, Durham, NC 27708, USA. [2]Department of Molecular Genetics, Utrecht University, Padualaan 8, 3584CH Utrecht, Netherlands.

*These authors contributed equally to this work.
†Present address: Max Planck Institute for Developmental Biology, Department of Genetics and Genomics, Spemannstrasse 35/III, D-72076 Tübingen, Germany.
‡Present address: Reproduction et Développement des Plantes Laboratory, Unité Mixte de Recherche 5667, Ecole Normale Supérieure de Lyon, 46, Alleé d'Italie, 69364 Lyon Cedex 07, France.
§Present address: Department of Biology, University of Pennsylvania, Philadelphia, PA 19104, USA.
‖To whom correspondence should be addressed. E-mail: philip.benfey@duke.edu

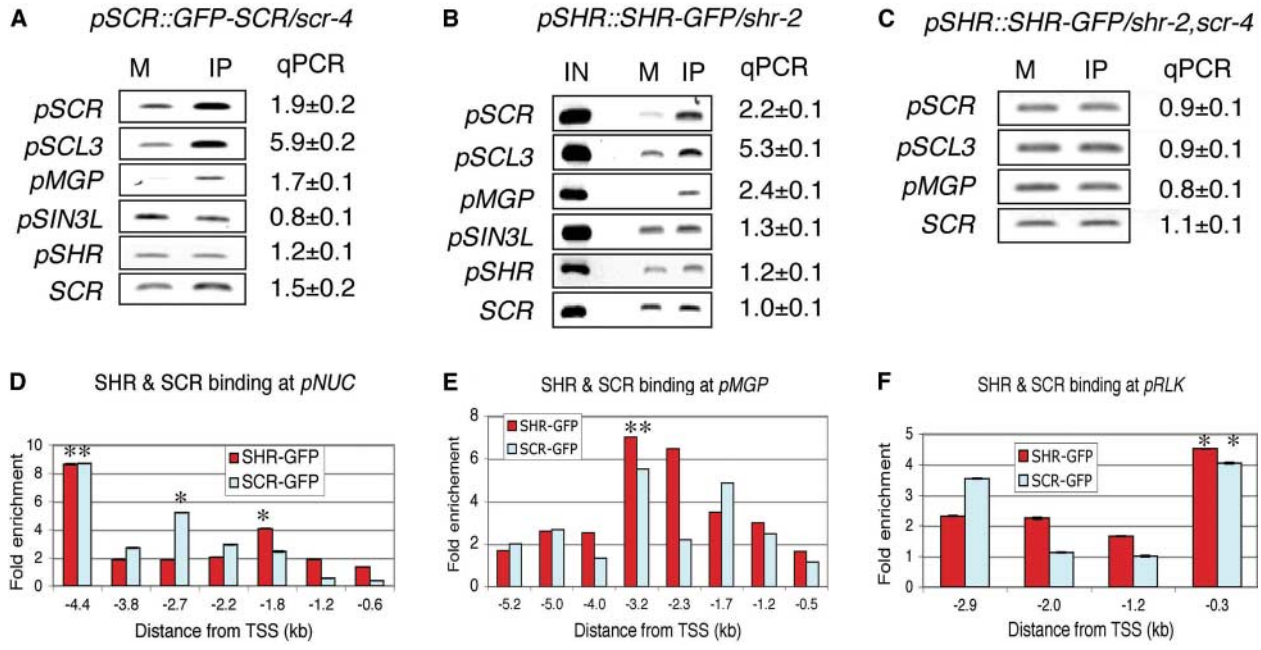

Fig. 1. SCR binds its own promoter and other SHR targets. (**A** and **B**) ChIP-PCR assay with the use of an antibody to GFP, showing binding by GFP-SCR and SHR-GFP to the promoters of *SCR*, *MGP*, and *SCL3*. Fold enrichment values in all panels, from (A) to (F), as determined by quantitative real-time PCR (QPCR), are means ± SE from technical replicates. *pSHR*, *SHR* promoter; *SCR*, *SCR* coding sequence; IN, input DNA; M, Mock ChIP. (**C**) SHR-GFP binding to some of its targets is abolished in *scr* mutant background. (**D** to **F**) SHR-GFP and GFP-SCR bind to the promoters of *NUC* (D), *MGP* (E), and *RLK* (F), as revealed by promoter scanning. The asterisks mark the positions of putative binding sites.

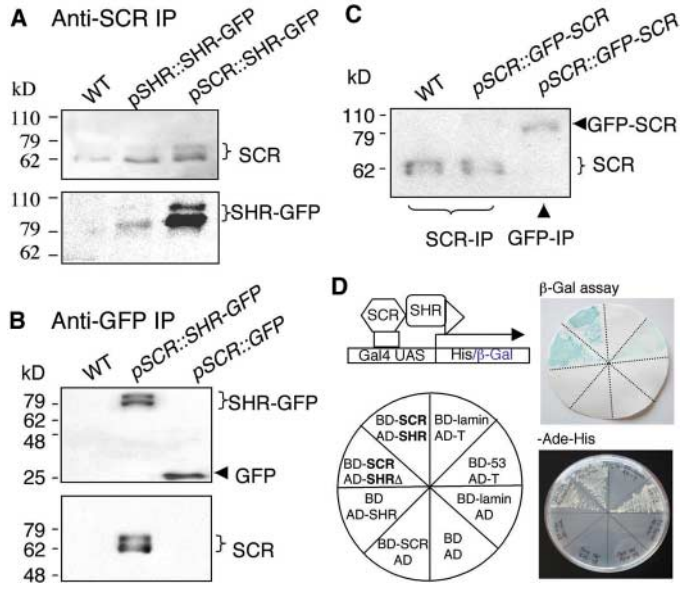

Fig. 2. SCR and SHR directly interact. (**A**) SHR-GFP is detected in SCR immunoprecipitates (SCR-IP). (**B**) SCR is coimmunoprecipitated with SHR-GFP. (**C**) SCR does not coimmunoprecipitate with GFP-SCR (GFP-IP). The SCR-IP assay shows that SCR is expressed in the transgenic plants expressing GFP-SCR. (**D**) Yeast two-hybrid assay showing direct interaction between SHR and SCR. AD-SHRΔ, which lacks the N-terminal 120 amino acids of SHR, still interacts with SCR. β-Gal, β-galactosidase; Gal4 UAS, Ga14 binding sites; BD, Ga14 DNA binding domain; AD, Ga14 activation domain; BD-53 and AD-T as a pair are used as a positive control, whereas the BD-lamin and AD-T pair is a negative control. BD-53, fusion between BD and the p53 protein; BD-lamin; fusion between BD and lamin; AD-T, fusion between AD and the T protein.

and the quiescent center (QC), and is required for the asymmetric cell division that gives rise to the cortex and endodermis (*3*, *7*). SHR protein does not move beyond a single layer comprising the endodermis, CEI cell, and QC. This is in sharp contrast to moving signal proteins in animals (*8*). Endodermis and cortex in the root are derived from the same initial cells through asymmetric cell divisions. Notably, although the number of cortex cell layers varies considerably, nearly all plant species examined so far have only one layer of endodermis, suggesting an evolutionarily conserved mechanism to form this single cell layer. SCR has been found to play a role in restricting SHR movement (*9*, *10*), but the underlying mechanism has remained unclear.

Positive feedback control of *SCR* transcription. SHR and SCR belong to the GRAS family of transcription factors (*11*). In both animals and plants, transcriptional regulation is known to play a key role in development (*12*, *13*). To elucidate the mechanism by which SHR and SCR control root radial patterning, we therefore first dissected their transcriptional circuits. Previously, it has been shown that SHR directly controls *SCR* transcription (*14*). However, there was also indication for SCR autoregulation (*9*). Using a chromatin immunoprecipitation–polymerase chain reaction (ChIP-PCR) assay (*15*), we found that SCR binds to its own promoter (Fig. 1A and fig. S2) but not to the promoters of *SHR* and a *SIN3*-like gene (*At5g15020*), which does not appear to be regulated by SHR (*14*). By reverse transcription PCR (RT-PCR), we confirmed the previous finding that *SCR* expression is reduced in both the *shr* and *scr* backgrounds (*9*) (fig. S2). Our results thus demonstrated that *SCR* is controlled by a SHR/SCR-dependent positive feedback loop.

SHR and SCR are functionally interdependent. Recently, we identified a number of additional putative direct targets of SHR (*14*). To determine whether these are also direct targets of SCR, we assayed binding by ChIP-PCR. Our initial results showed that SCR binds to the promoters of *MAGPIE* (*MGP*) and *SCR-LIKE 3* (*SCL3*) (Fig. 1A and fig. S3), which are also bound by SHR (Fig. 1B and fig. S3). We then checked SHR and SCR binding to other putative direct SHR targets by promoter scanning (*15*) (Fig. 1 and fig. S4). We found that SHR and SCR both clearly bind to the promoters of *NUTCRACKER* (*NUC*), a receptor-like kinase (RLK), and *MGP* (Fig. 1, D to F). Their binding

Table 1. Expression levels of SHR direct targets in *shr* and *scr* mutants, relative to WT, as measured by whole-genome Affymetrix ATH1 microarray. FC, fold change (reduction).

	shr (FC)	*P* value	*scr* (FC)	*P* value
NUC	2.8	6.4×10^{-27}	1.6	9.2×10^{-5}
MGP	2.5	3.7×10^{-19}	1.5	1.7×10^{-3}
SCR	2.5	5.0×10^{-8}	4.0	4.3×10^{-7}
Br6ox2	1.9	7.4×10^{-23}	1.8	3.0×10^{-4}
RLK	1.4	2.8×10^{-5}	1.4	3.8×10^{-1}
SCL3	1.3	6.3×10^{-3}	1.4	7.6×10^{-2}
Tropinone reductase (*TRI*)	1.2	2.7×10^{-1}	1.2	7.0×10^{-1}
SNEEZY (*SNE*)	1.0	6.6×10^{-1}	0.8	5.9×10^{-5}

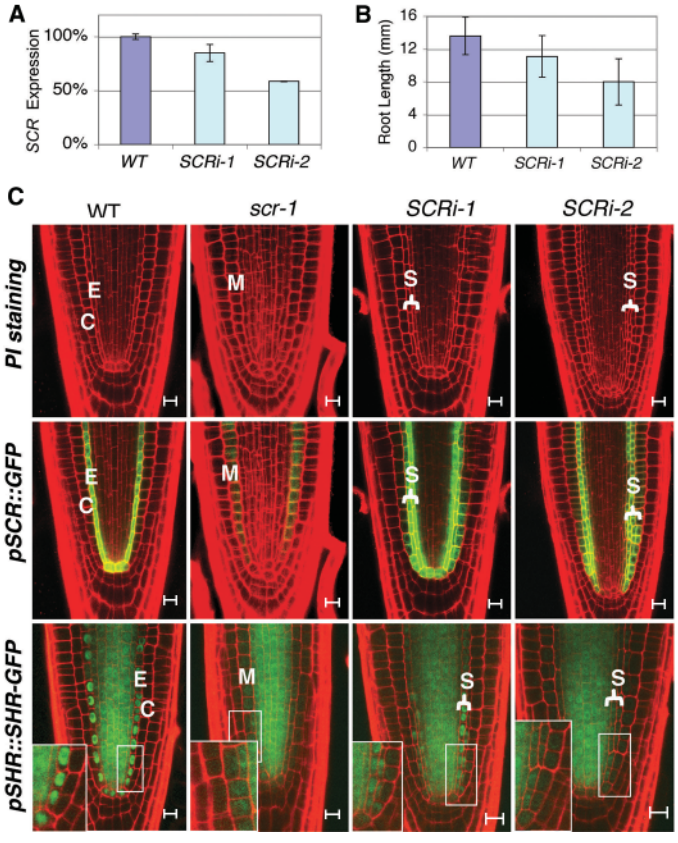

Fig. 3. SCR determines SHR subcellular localization and its range of movement. (**A**) *SCR* transcript levels in two independent *SCR* RNAi lines (*SCRi-1* and *SCRi-2*), relative to that in WT, as determined by RT-QPCR. (**B**) Root lengths of the *SCR* RNAi lines and WT 6 days after germination. Error bars in (A) and (B) indicate SD. (**C**) Confocal images of 6-day-old roots of WT, *scr-1*, *SCRi-1*, and *SCRi-2* seedlings, showing their structure [propidium iodide (PI) staining], an endodermal marker expression (*pSCR::GFP*), and SHR-GFP localization (*pSHR::SHR-GFP*). The insets in the bottom panels are enlarged images of the framed areas. C, cortex; E, endodermis; M, mutant cell layer; S, supernumerary cell layers. Scale bars, 10 μm.

sites on the *NUC* and *MGP* promoters were located in regions relatively far upstream of the translation start sites (TSS) (Fig. 2, D and E), which explains why we were unable to confirm *NUC* as a direct SHR target by ChIP-PCR using PCR primers that amplify more proximal sequences (*14*). Notably, most binding sites for SHR and SCR at these promoters appear to coincide.

The observation that SHR and SCR bind to a common set of genes suggests functional interdependence between these two transcriptional regulators. We therefore examined SHR binding to some of its targets in an *scr* background. In the absence of SCR, SHR binding to these targets is abolished (Fig. 1C). Expression levels of all these genes are reduced in the *shr* and *scr* mutants (fig. S2), indicating that SCR is required for SHR to regulate these genes. To determine the extent of overlap between SHR and SCR targets, we performed genome-wide expression analysis in *shr* and *scr* mutants. Nearly all putative direct SHR targets that we previously identified (*14*) show significant reduction in their expression in both mutant backgrounds (Table 1). Moreover, a large portion of SHR indirect targets also showed reduced expression in the *scr* background (table S1).

SHR and SCR proteins directly interact. Functional interdependence between SHR and SCR could be achieved through their cooperative binding to the same promoter or through direct interaction. To determine whether SHR and SCR form a complex, we performed coimmunoprecipitation. Reciprocal pull-down experiments showed that SCR and SHR are in a complex (Fig. 2, A and B). In yeast cells, SHR and SCR interact directly (Fig. 2D), and the central domain spanning the two leucine heptad repeats and the VHIID (Val-His-Ile-Ile-Asp) motif is responsible for this interaction (fig. S5). However, SCR does not appear to interact with itself (Fig. 2C). The finding that SCR physically interacts with SHR provides a molecular basis for their functional interdependence. However, clearly not all aspects of SHR activity rely on interaction with SCR, because the mutant ground-tissue layer in *scr* still expresses endodermal markers that are not detected in the *shr* mutant background. One hypothesis is that the SHR/SCR complex controls some aspects of SHR function, such as asymmetric cell division, QC specification, and stem cell maintenance, whereas complexes formed between SHR and other proteins fulfill other aspects of SHR function, particularly endodermis specification.

SCR affects SHR subcellular localization and movement. As the SHR protein with a strong nuclear localization signal is no longer capable of moving (*7*), the finding that SHR and SCR directly interact suggests that one role for SCR might be to sequester SHR into the nucleus, thus preventing its movement. Indeed, the fusion protein between green fluorescent protein (GFP) and SHR (SHR-GFP) becomes largely cytoplasmic in the mutant cell layer of *scr* (*scr-1* in Fig. 3C) (*10*), in contrast to its exclusive nuclear localization in the endodermis of wild-type (WT) roots (Fig. 3C). However, because of the low amount of SHR-GFP in the mutant cell layer, it is unclear whether SHR moves out of the mutant layer into the epidermis.

A large pool of SCR would be required to completely block SHR movement. The positive feedback loop for SCR transcription could provide such a mechanism (*16*). To test this hypothesis, we examined the effect of reduction in SCR expression on SHR movement using an RNA interference (RNAi) construct. We reasoned that, if SCR levels were reduced below a threshold level, some SHR protein might be able to move into the presumptive cortex where it would activate *SCR* transcription and endodermis specification. Asymmetric cell division would also occur, giving rise to an additional layer of ground tissue. This process could be repeated until free-moving SHR was exhausted. In support of our hypothesis, plants from the RNAi transgenic lines that we generated produced multiple layers of cells. Two lines that have different levels of *SCR* transcript were further examined (Fig. 3A). As shown in Fig. 3C, the extra cell layers in both lines express the endodermal marker *pSCR::GFP*, and SHR-GFP expressed in the stele is also present in these supernumerary cell layers. Notably, SHR-GFP is detected in both daughter cells of the CEI cell, whereas its levels appear to decrease in the outer cell layer after each additional cell division (Fig. 3C, insets). Moreover, the number of supernumerary cell layers is inversely correlated with the level of *SCR* transcript in the two independent transgenic lines. Furthermore, SHR-GFP is primarily nuclear-

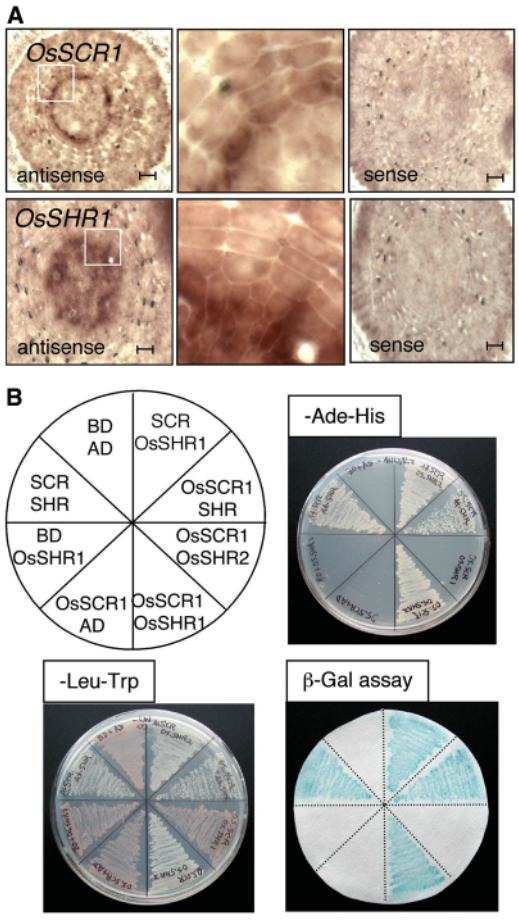

Fig. 4. Analysis of *SHR* and *SCR* homologs from rice. (**A**) In situ hybridization showing the expression patterns of *OsSCR1* and *OsSHR1* in rice root. The framed areas in the left panels are shown at a higher magnification (middle panels). Scale bars, 20 μm. (**B**) Yeast two-hybrid assay examining the interaction between OsSHR1 or OsSHR2 with OsSCR1, as well as their interaction with SHR and SCR. Ade, adenine.

localized in the supernumerary layers of *SCRi-1*, the weaker RNAi line, but is largely cytoplasm-localized in *SCRi-2*, the stronger RNAi line (Fig. 3C). The two lines also showed reduced root length that correlates with the strength of RNAi (*P* values are 2.9×10^{-5} and 2.8×10^{-13}, respectively; Student's *t* test, $n = 39$ roots), although the QC, CEI, and other initials appear normal (Fig. 3, A and B). These results demonstrate the critical role of the positive feedback mechanism for SCR in restricting SHR movement, root radial patterning, and root growth.

Our results support a mechanism by which SCR tightly restricts SHR movement, as described below. On the one hand, SCR sequesters SHR into the nucleus through protein complex formation, making SHR incapable of further movement. On the other hand, the SHR/SCR-dependent positive feedback loop for *SCR* transcription ensures no free-moving SHR can escape from the endodermis by driving a rapid buildup of SCR that does not self-interact but rather preferentially interacts with SHR. This mechanism would require a basal level of SCR expression to initiate the feedback loop. Notably, a substantial level of *SCR* mRNA is still detectable in both the *shr* and *scr* backgrounds, and its specific radial expression pattern is largely unaltered. This SHR/SCR-independent basal *SCR* transcription may be one of the key factors defining the boundary for SHR movement.

The model that we propose for SCR to restrict SHR movement could also account for the fact that different cell fates are rapidly acquired by the progeny of the daughter cells of the CEI cell (*9*). After this asymmetric cell division, the concentration of the SHR/SCR complex will remain high in the inner cell of the endodermal lineage driven by a sustained supply of SHR from the stele, which activates the SCR feedback loop. This high concentration of the SHR/SCR complex would maintain the expression of SCR as well as other downstream patterning genes. By contrast, the SHR/SCR concentration in the other cell of the cortex lineage would drop rapidly, resulting from the inability of SHR to move beyond the endodermis coupled with protein turnover and the dilution accompanying cell division. Indeed, although SCR is detected in both cells immediately after the asymmetric cell division, *SCR* and other endodermal markers are only expressed in the endodermis soon thereafter (*9*).

Interaction and expression of SHR and SCR homologs in rice. The observations that nearly all plants examined so far have only a single layer of endodermis (even though the number of cortex layers can be highly variable) and that *SCR* orthologs are exclusively expressed in the endodermis (*17*–*19*) suggest that the mechanism described above is likely to be evolutionarily conserved. However, the only *SHR* homolog cloned so far, which is claimed to be the closest *SHR* homolog from rice, shows an expression pattern that is distinct from *SHR* in *Arabidopsis* (*19*), thus casting doubt on this hypothesis.

Database searches revealed that there are, in fact, two close rice homologs for both *SHR* (*Os03g31750* and *Os07g39820*) and *SCR* (*Os11g03110* and *Os12g02870*). We named the more similar SHR and SCR homologs OsSHR1 (*Os07g39820*) and OsSCR1 (*Os11g03110*) and the more dissimilar ones OsSHR2 (*Os03g31750*) and OsSCR2 (*Os12g02870*), respectively (table S2).

The rice genes that were previously reported as homologs of *SHR* and *SCR* are *OsSHR2* and *OsSCR1* (*19*). We therefore cloned *OsSHR1* and analyzed its expression in rice roots by in situ hybridization. As shown in Fig. 4A, *OsSHR1* and *OsSCR1* are both expressed in tissues analogous to those of their counterparts in *Arabidopsis*. OsSCR1 and OsSHR1 interact in yeast as strongly as *Arabidopsis* SHR and SCR do (Fig. 4B). They also interact equally well with SHR and SCR, but no interaction was observed between OsSHR2 and OsSCR1 (Fig. 4B). These results strongly suggest that *OsSHR1* and *OsSCR1* are functional homologs of *SHR* and *SCR* in rice. They further suggest that the functional relationship between SHR and SCR, as well as their role in radial patterning in higher plants, is evolutionarily conserved.

Proteins that move as signaling molecules play a critical role in both animal and plant development (*8*, *20*, *21*). Although the list of transcription factors that are able to move is growing (*22*–*28*), little is known about the mechanisms regulating intercellular movement. Decapentaplegic (Dpp), for example, a well-characterized example from animals, moves passively by diffusion and forms a gradient across multiple layers of cells as a result of unregulated binding to and internalization by its receptors located on the surface of the cells that it passes through (*8*, *29*). By contrast, both SHR movement and its range of action are actively regulated, and the mechanism that we have uncovered in this study is quite distinct from those previously described. Although some aspects of this mechanism have been reported for other proteins, this is the first example where both protein-protein interaction and transcriptional control are involved to achieve tight control of protein movement. This difference may extend to other moving plant proteins and indicate a fundamental difference between plant and animal signaling during development.

References and Notes

1. L. Dolan *et al.*, *Development* **119**, 71 (1993).
2. Y. Helariutta *et al.*, *Cell* **101**, 555 (2000).
3. L. Di Laurenzio *et al.*, *Cell* **86**, 423 (1996).
4. S. Sabatini, R. Heidstra, M. Wildwater, B. Scheres, *Genes Dev.* **17**, 354 (2003).
5. B. Scheres *et al.*, *Development* **121**, 53 (1995).
6. K. Nakajima, G. Sena, T. Nawy, P. N. Benfey, *Nature* **413**, 307 (2001).
7. K. L. Gallagher, A. J. Paquette, K. Nakajima, P. N. Benfey, *Curr. Biol.* **14**, 1847 (2004).

8. T. Y. Belenkaya *et al.*, *Cell* **119**, 231 (2004).
9. R. Heidstra, D. Welch, B. Scheres, *Genes Dev.* **18**, 1964 (2004).
10. G. Sena, J. W. Jung, P. N. Benfey, *Development* **131**, 2817 (2004).
11. L. D. Pysh, J. W. Wysocka-Diller, C. Camilleri, D. Bouchez, P. N. Benfey, *Plant J.* **18**, 111 (1999).
12. M. Levine, E. H. Davidson, *Proc. Natl. Acad. Sci. U.S.A.* **102**, 4936 (2005).
13. P. N. Benfey, D. Weigel, *Plant Physiol.* **125**, 109 (2001).
14. M. P. Levesque *et al.*, *PLoS Biol.* **4**, e143 (2006).
15. Materials and methods are available as supporting material on *Science* Online.
16. H. Kitano, *Nat. Rev. Genet.* **5**, 826 (2004).
17. N. Sassa, Y. Matsushita, T. Nakamura, H. Nyunoya, *Plant Cell Physiol.* **42**, 385 (2001).
18. J. Lim *et al.*, *Plant Cell* **12**, 1307 (2000).
19. N. Kamiya, J. Itoh, A. Morikami, Y. Nagato, M. Matsuoka, *Plant J.* **36**, 45 (2003).
20. M. Strigini, *J. Neurobiol.* **64**, 324 (2005).
21. K. L. Gallagher, P. N. Benfey, *Genes Dev.* **19**, 189 (2005).
22. J. Y. Lee *et al.*, *Science* **299**, 392 (2003).
23. J. Y. Lee *et al.*, *Proc. Natl. Acad. Sci. U.S.A.* **103**, 6055 (2006).
24. T. Kurata *et al.*, *Development* **132**, 5387 (2005).
25. X. Wu *et al.*, *Development* **130**, 3735 (2003).
26. D. Rogulja, K. D. Irvine, *Cell* **123**, 449 (2005).
27. J. Y. Kim, Z. Yuan, M. Cilia, Z. Khalfan-Jagani, D. Jackson, *Proc. Natl. Acad. Sci. U.S.A.* **99**, 4103 (2002).
28. C. Weinl *et al.*, *Plant Cell* **17**, 1704 (2005).
29. Y. C. Wang, E. L. Ferguson, *Nature* **434**, 229 (2005).
30. We thank X. Dong (Duke University) for the *p35S::GFP* plants, and D. McClay, Z.-M. Pei, R. Heidstra, and members of the Benfey Laboratory for critical reading of the manuscript and helpful comments. We acknowledge fellowship support from the Human Frontiers Science Program and the European Molecular Biology Organization (for T.V.), NIH (for A.J.P.), and NSF (for M.P.L.). This work was supported by a grant to P.N.B. from NIH (RO1-GM043778).

Supporting Online Material

www.sciencemag.org/cgi/content/full/316/5823/421/DC1
Materials and Methods
Figs. S1 to S5
Tables S1 to S3
References

4 January 2007; accepted 6 March 2007
10.1126/science.1139531

Nonequilibrium Phase Transitions in Cuprates Observed by Ultrafast Electron Crystallography

Nuh Gedik,[1] Ding-Shyue Yang,[1] Gennady Logvenov,[2] Ivan Bozovic,[2] Ahmed H. Zewail[1]*

Nonequilibrium phase transitions, which are defined by the formation of macroscopic transient domains, are optically dark and cannot be observed through conventional temperature- or pressure-change studies. We have directly determined the structural dynamics of such a nonequilibrium phase transition in a cuprate superconductor. Ultrafast electron crystallography with the use of a tilted optical geometry technique afforded the necessary atomic-scale spatial and temporal resolutions. The observed transient behavior displays a notable "structural isosbestic" point and a threshold effect for the dependence of *c*-axis expansion (Δc) on fluence (F), with $\Delta c/F = 0.02$ angstrom/(millijoule per square centimeter). This threshold for photon doping occurs at ~0.12 photons per copper site, which is unexpectedly close to the density (per site) of chemically doped carriers needed to induce superconductivity.

The physical and chemical properties of materials can be altered as a result of the generation of metastable structures (*1*), electronic and/or structural modifications (*2*, *3*), and phase transitions (*4*). For the latter, much of the work has been done on solids at equilibrium, namely when temperature or pressure becomes the variable of change. In contrast, transient structures of nonequilibrium phases, which are formed by collective interactions, are elusive and less studied because they are inaccessible to conventional studies of the equilibrium state. Initiated by photons, the structural changes underlying such transitions involve charge redistribution and lattice relaxation, culminating in a process termed a photoinduced phase transition (*5*–*7*). In order to understand the nature of these optically dark phases, it is important to observe the structural changes with the use of time-resolved methods, especially those that use ultrafast electron microscopy (*8*–*10*), electron diffraction (*10*–*12*), and x-ray absorption and diffraction (*13*–*17*). Here, the direct observation of the nonequilibrium structural phase transition in superconducting cuprates is reported.

We have previously established ultrafast electron crystallography (UEC) (*10*) as a method for studying surfaces and nanometer-scale materials with atomic-scale resolutions. Our apparatus integrates a femtosecond laser system into an ultrahigh vacuum (UHV) assembly of three chambers (Fig. 1A). In this technique, the output of a Ti:sapphire femtosecond laser (with a pulse width of 120 fs) is split into two beams: an 800-nm pulse used to excite the sample and a 266-nm pulse (generated by frequency tripling) used to produce an electron packet via the photoelectric effect. The electrons are then accelerated at 30 kV, resulting in a de Broglie wavelength of $\lambda = 0.07$ Å. The diffraction patterns of these electrons from the sample are recorded on a charge-coupled device (CCD) camera with single-electron sensitivity. The time delay between the initiating laser pulse and electron probe packet is controlled by changing the optical path length between the two pulses. Diffraction patterns at different delay times (diffraction frames) provide a movie of structural change, with atomic-scale spatial and ultrashort temporal resolutions (*10*, *18*).

The material that we chose to study is oxygen-doped $La_2CuO_{4+\delta}$; although the undoped material is an antiferromagnetic Mott insulator, doping confers superconductivity below the critical temperature (T_c) and metallic properties at room temperature. Thin films were grown on a $LaSrAlO_4$ substrate by means of an atomic-layer molecular beam epitaxy system (*19*). The films under study were characterized during growth by reflection high-energy electron diffraction and ex situ by atomic force microscopy (AFM), x-ray diffraction (XRD), and measurements of resistivity and magnetic susceptibility as a function of temperature (*20*).

In order to observe lower-order Bragg diffractions from the material, the incident angle of electrons ($\theta/2$) is set typically between ~1° and 2°. Because the speed of electrons is about one-third that of light, a large group-velocity mismatch occurs between the laser pulse and the electron packet. Moreover, the electron beam has, at this angle of incidence, a large footprint on the surface of the material: in this case, the (001) planes with the *c* axis defining the surface normal direction. We have implemented a wavefront tilting scheme,

[1]Physical Biology Center for Ultrafast Science and Technology, California Institute of Technology (Caltech), Pasadena, CA 91125, USA. [2]Brookhaven National Laboratory (BNL), Upton, NY 11973–5000, USA.

*To whom correspondence should be addressed. E-mail: zewail@caltech.edu

ERRATUM

Post date 21 December 2007

Research Articles: "An evolutionarily conserved mechanism delimiting SHR movement defines a single layer of endodermis in plants" by H. Cui *et al*. (20 April 2007, p. 421). In two instances in the fifth paragraph on page 424, one of the rice homologs for *SHR*, *Os03g31880*, was mistyped as *Os03g31750*.